

ANALYTICAL MODELING OF THE HIGH STRAIN RATE DEFORMATION OF POLYMER MATRIX COMPOSITES

Robert K. Goldberg
AIAA Senior Member
Aerospace Engineer
NASA Glenn Research Center
Cleveland, OH 44135, U.S.A.

Gary D. Roberts
Aerospace Engineer
NASA Glenn Research Center
Cleveland, OH 44135, U.S.A.

Amos Gilat
Professor
Mechanical Engineering Department
The Ohio State University
Columbus, OH 43210, U.S.A.

Abstract

The results presented here are part of an ongoing research program to develop strain rate dependent deformation and failure models for the analysis of polymer matrix composites subject to high strain rate impact loads. State variable constitutive equations originally developed for metals have been modified in order to model the nonlinear, strain rate dependent deformation of polymeric matrix materials. To account for the effects of hydrostatic stresses, which are significant in polymers, the classical J_2 plasticity theory definitions of effective stress and effective plastic strain are modified by applying variations of the Drucker-Prager yield criterion. To verify the revised formulation, the shear and tensile deformation of a representative toughened epoxy is analyzed across a wide range of strain rates (from quasi-static to high strain rates) and the results are compared to experimentally obtained values. For the analyzed polymers, both the tensile and shear stress-strain curves computed using the analytical model correlate well with values obtained through experimental tests. The polymer constitutive equations are implemented within a strength of materials based micromechanics method to predict the nonlinear, strain rate dependent deformation of polymer matrix composites. In the micromechanics, the unit cell is divided up into a number of independently analyzed slices, and laminate theory is then applied to obtain the effective deformation of the unit cell. The composite mechanics are verified by analyzing the deformation of a representative polymer matrix composite (composed using the representative polymer analyzed for the

correlation of the polymer constitutive equations) for several fiber orientation angles across a variety of strain rates. The computed values compare favorably to experimentally obtained results.

Introduction

NASA Glenn Research Center has an ongoing research program to develop computational methods for the analysis of polymer matrix composites subject to high strain rate impact loads. Under these types of loading conditions, the deformation of the composite can be highly strain rate dependent and nonlinear, which must be accounted for within the analytical model. The deformation of polymer composites is ordinarily assumed to be linear elastic and independent of strain rate in transient dynamic finite element codes used for impact analysis.¹

Polymers are known to have a strain rate dependent deformation response that is nonlinear above about one or two percent strain. Traditionally, viscoelasticity models have been used to capture this behavior.² However, there has been an interest in the research community in using constitutive equations developed for metals, based on plasticity and viscoplasticity approaches, to model the nonlinear, strain rate dependent behavior of polymers and polymer matrix composites. For example, Sun and co-workers^{3,4} developed a macromechanical, transversely isotropic plasticity theory to analyze the nonlinear deformation of polymer composites. Bordonaro⁵ adapted the viscoplasticity theory based on overstress, originally developed for metals, to analyze the nonlinear deformation of Nylon 66. Pan and co-workers^{6,7} and

¹ This is a preprint or reprint of a paper intended for presentation at a conference. Because changes may be made before formal publication, this is made available with the understanding that it will not be cited or reproduced without the permission of the author.

Hsu, et al⁸ developed viscoplasticity theories to analyze the nonlinear deformation of polymers including the effects of hydrostatic stresses. In these cases, the effects of hydrostatic stresses on the nonlinear deformation, which unlike in metals are significant for polymers⁹, were accounted for by applying variations of the Drucker-Prager yield criterion¹⁰ to modify the definitions of the effective stress and the effective plastic strain. A preliminary effort to account for the hydrostatic stress effects on the high strain rate deformation of polymers was carried out by the authors of this report¹¹.

In this paper, constitutive equations are developed to analyze the nonlinear, strain rate dependent deformation of polymeric matrix materials in which the effects of hydrostatic stresses on the nonlinear deformation response are properly accounted for. The equations developed in previous work¹¹ were modified in order to more accurately simulate the multiaxial stress states found in a composite material. The tensile and shear deformation of a representative toughened epoxy polymer is characterized and modeled. The implementation of the polymer constitutive equations within a mechanics of materials based micromechanics model incorporating a fiber substructuring approach is presented, which permits the analysis of the strain rate dependent, nonlinear deformation of polymer matrix composites. The tensile deformation of a carbon fiber reinforced polymer matrix composite composed using the representative polymer examined for the correlation of the polymer constitutive equations will be analyzed and compared to experimentally obtained results.

Polymer Constitutive Equations

To analyze the nonlinear, strain rate dependent deformation of the polymer matrix, the Bodner-Partom viscoplastic state variable model¹², which was originally developed for metals, is modified. In state variable models, there is no defined yield stress; inelastic strains are assumed to be present at all stress levels. In the “elastic” range of deformation, the inelastic strains are assumed to be very small. State variables, which evolve with stress and inelastic strain, are defined to represent the average effects of the deformation mechanisms.

For this study, temperature effects are neglected, and phenomena such as creep, relaxation and high cycle fatigue are not accounted for within the equations. The nonlinear strain recovery observed in polymers on unloading is not currently simulated, and small strain theory is assumed to apply. An important point to note is that in the original Bodner model as applied to metals each of the state variables and material constants had a

fairly explicit link to specific deformation mechanisms. In the application of the applications to the analysis of polymers, the relationship of the various constants and variables to specific deformation mechanisms is somewhat more phenomenological. Furthermore, all of the nonlinearity and strain rate dependence is assumed to be due to irreversible deformations. In reality, the nonlinear deformation is most likely a combination of damage, reversible deformation mechanisms and irreversible deformation mechanisms. However, as will be shown, for the deformation modes examined in the study the model as presented appears to do an adequate job of simulating the nonlinear, strain rate dependent deformation of the polymers examined. Furthermore, the presented model employs a fairly simple formulation with a minimum of material constants which are fairly easily obtained.

In the modified Bodner-Partom model used for this study, the components of the inelastic strain rate $\dot{\varepsilon}_{ij}^I$ are defined as a function of the deviatoric stress components s_{ij} , the second invariant of the deviatoric stress tensor J_2 and an isotropic state variable Z which represents the resistance to molecular flow in the polymer (internal stress) in the form

$$\dot{\varepsilon}_{ij}^I = D_o \exp \left[-\frac{1}{2} \left(\frac{Z}{\sigma_e} \right)^{2n} \right] \left(\frac{s_{ij}}{\sqrt{J_2}} + \frac{2\alpha}{3\sqrt{3}} \delta_{ij} \right) \quad (1)$$

where α is a state variable controlling the level of the hydrostatic stress effects and D_o and n are material constants. D_o represents the maximum inelastic strain rate, and n controls the rate dependence of the material. The elastic components of strain are added to the inelastic strain to obtain the total strain. The term σ_e represents the effective stress state in the material, and was modified from the original formulation¹¹ in order to account for the effects of hydrostatic stresses in a polymeric material. Based on the formulation used by Chang and Pan⁷ and Hsu, et al⁸, the effective stress is defined as follows in this work in order to account for the effects of hydrostatic stresses

$$\sigma_e = \sqrt{3J_2} + \alpha \sigma_{kk} \quad (2)$$

where σ_{kk} is the summation of the normal stress components (equal to three times the hydrostatic stress). This formulation of the effective stress is based on the Drucker-Prager yield criteria¹⁰. Under pure shear loading, the hydrostatic stress is equal to zero and the equation reduces to the original formulation¹², in which

the effective stress was set equal to $\sqrt{3J_2}$ for all loading conditions.

The rate of evolution of the internal stress state variable Z and the mean stress effect state variable α are defined by the equations

$$\dot{Z} = q(Z_1 - Z)\dot{\epsilon}_e^I \quad (3)$$

$$\dot{\alpha} = q(\alpha_1 - \alpha)\dot{\epsilon}_e^I \quad (4)$$

where q is a material constant representing the "hardening" rate, and Z_1 and α_1 are material constants representing the maximum values of Z and α , respectively. The initial values of Z and α are defined by the material constants Z_0 and α_0 .

The term $\dot{\epsilon}_e^I$ in Equations 3 and 4 represents the effective deviatoric inelastic strain rate, defined as follows

$$\begin{aligned} \dot{\epsilon}_e^I &= \sqrt{\frac{2}{3}\dot{\epsilon}_{ij}^I\dot{\epsilon}_{ij}^I} \\ \dot{\epsilon}_{ij}^I &= \dot{\epsilon}_{ij}^I - \dot{\epsilon}_m^I \end{aligned} \quad (5)$$

where $\dot{\epsilon}_{ij}^I$ are the components of the inelastic strain rate tensor and $\dot{\epsilon}_m^I$ is the mean inelastic strain rate. In the original Bodner model¹², the total inelastic strain and strain rate are used in the evolution law and are assumed to be equal to their deviatoric values. As discussed by Li and Pan⁶, since hydrostatic stresses contribute to the inelastic strains in polymers, indicating volumetric effects are present, the mean inelastic strain rate cannot be assumed to be zero, as is the case in the inelastic analysis of metals. An important point to note is that in the original Bodner model¹¹, the inelastic work rate was used instead of the effective inelastic strain rate in the evolution equation for the internal stress state variable. However, for this work the inelastic strain rate was deemed easier to work with from both computational and characterization points of view, particularly in the incorporation of hydrostatic stress effects. Since hydrostatic stress effects were not considered in the original Bodner model¹¹, the evolution equation for α is a new addition to the formulation. The state variable α is assumed to evolve in the same manner as the state variable Z. By using this assumption the value of q used in Equation 3 will be the same as the value of q used in Equation 4.

Details on how to obtain the material constants can be found in Goldberg, Roberts and Gilat¹¹.

Polymer Equations Correlation Studies

A series of shear stress-shear strain curves and tensile stress-strain curves have been experimentally generated for a representative toughened epoxy resin, 977-2. The shear tests were conducted at strain rates of approximately 9×10^{-5} /sec, 2 /sec and 500 /sec. The tensile tests were conducted at strain rates of approximately 5.7×10^{-5} /sec, 1 /sec and 365 /sec. The low strain rate tests were conducted using an Instron hydraulic testing machine. The high strain rate tests were conducted using a split Hopkinson bar. The material constants for the constitutive model were primarily determined using the shear data. The tensile data were used to determine the initial and final values of α . The material constants, determined using the procedures described in Goldberg, Gilat and Roberts¹¹, are as follows: E=3500 MPa, v=0.40, $D_0=1 \times 10^6$, n=0.73, $Z_1=1546$ MPa, $Z_0=380$ MPa, q=101, $\alpha_1=0.201$, $\alpha_0=0.223$.

Experimental and predicted shear stress-strain curves are shown in Figure 1 and uniaxial tensile stress-strain curves are shown in Figure 2 for the 977-2 material. As can be seen in the figures, for both tensile and shear loading the material has a strain rate dependent, nonlinear deformation response. For the shear test at high strain rates, the sharp increase in stress at the beginning of the loading with negligible increase in strain is most likely the result of a lack of stress equilibrium at the start of loading. The oscillations seen in the tensile response at high strain rates are most likely due to the specimen geometry leading to the stress waves being visible in the response.

The predicted results match the experimental values reasonably well for all strain rates for both tensile and shear loading. For the medium strain rate, the stresses are slightly underpredicted for the initial portion of the nonlinear section of the stress-strain curve. This discrepancy may be due to the fact that the values of all of the material constants were assumed not to vary with strain rate. In actuality, this assumption may not be completely accurate. While not shown here, as discussed in Goldberg, Gilat and Roberts¹¹ if the hydrostatic stress effects are not properly accounted for and the material is characterized based on the shear results, the predicted stresses under tensile loading would be much higher than the experimental values in the nonlinear range. Furthermore, if the value of the mean stress effect state variable α was kept constant at its final value, the stresses in the early part of the loading curve would be over predicted. This result is significant in that in previous efforts in the literature to

account for the effects of mean stresses in the deformation response of polymers, the effects of the hydrostatic stresses have been assumed to be constant over the entire range of loading.

Composite Micromechanical Modeling

Micromechanical techniques are used to predict the effective properties and deformation response of the individual plies in a composite laminate. The effective properties and deformation response are computed based on the properties of the individual constituents. Lamination theory can then be used to compute the effective deformation response of the entire composite. The constitutive equations described above have been implemented within a micromechanics method in order to enable the prediction of the nonlinear, strain rate dependent deformation response of polymer matrix composites with the effects of hydrostatic stresses incorporated into the analysis. The micromechanics method has been described extensively in Goldberg¹³. A summary of the methodology will be given here.

For this work the unit cell, the smallest material unit for which the response can be considered to be representative of the entire composite ply, is defined to consist of a single fiber and its surrounding matrix. Due to symmetry, only one-quarter of the unit cell was analyzed. The composites are assumed to have a periodic, square fiber packing and a perfect interfacial bond is specified. The fibers are assumed to be transversely isotropic and linear elastic with a circular cross-section. The matrix is assumed to be isotropic, with a rate dependent, nonlinear deformation response computed using the equations described in the previous section of this report. A key assumption of this approach is that the in-situ matrix properties are equivalent to the bulk properties of the polymer. However, the advantage of using this type of methodology is that it is simpler to conduct experiments on the pure resin and to determine the material constants from the pure resin data as opposed to trying to back out the resin properties from composite test data. Furthermore, a key goal of this research is to provide a methodology that facilitates reducing the amount of testing of the composite that is required to obtain strain rate dependent material properties that can be input into a finite element code. Conducting strain rate dependent tensile tests on the pure resin and using that data to predict the composite deformation response is also much simpler than conducting tests on the composite. However, if in comparing test data obtained from composite specimens to analytical predictions it appears that the bulk matrix properties do not accurately reflect the in-situ state of the matrix, the polymer properties can always be appropriately adjusted.

The unit cell is divided up into an arbitrary number of rectangular, horizontal slices of equal thickness, as is shown in Figure 3. Similar approaches have been used by researchers such as Whitney¹⁴, Greszczuk¹⁵ and Mital, et al¹⁶. Each slice is assumed to be in a state of plane stress. This assumption is made based on the fact that laminate theory will be applied to each ply of the composite laminate, which implies that the unit cell and every slice within the unit cell is in a state of plane stress. The top and bottom slices in the unit cell are composed of pure matrix. The remaining slices are composed of two subslices; one composed of fiber material and the other composed of matrix material. For the slices containing both fiber and matrix, the out-of-plane stresses can be nonzero in individual subslices, but the volume average of the out-of-plane stresses must be equal to zero. By using this approach, the behavior of each slice is decoupled, and the response of each slice can be determined independently, which significantly reduces the level of complexity in the analysis. Laminate theory is then used to obtain the effective response of the unit cell.

The thickness, fiber volume ratio and thickness ratio (the ratio of the slice thickness to the total unit cell thickness) for each slice can be determined using the composite fiber volume ratio and geometric principles. The unit cell is assumed to measure one unit in length by one unit in height. The first step is to compute the area of the cross-section of the fiber within each slice. The overall diameter of the fiber (d_f) is related to the fiber volume fraction of the overall composite (V_f) through the following relationship

$$d_f = \sqrt{\frac{4V_f}{\pi}} \quad (6)$$

and this term can be used along with the standard geometric definition of the radius of a circle to compute the horizontal coordinate of any point on the outer surface of the fiber in terms of the fiber volume fraction and the vertical coordinate. The area of the portion of the fiber contained within each slice (A_f^i) within the one-quarter of the unit cell which is analyzed can be computed by integrating the resulting expression between the vertical (z) coordinates of the top and bottom of slice "i"

$$A_f^i = \int_{z_{i-1}}^{z_i} \sqrt{\frac{V_f}{\pi} - z^2} dz \quad (7)$$

which is also the equivalent area of the rectangular fiber slice in the portion of the unit cell which is analyzed (one-quarter due to symmetry).

The fiber volume fraction of each slice composed of fiber and matrix is equal to the fiber area in each slice divided by the total slice area. The thickness ratio for each slice composed of both fiber and matrix is equal to the slice thickness divided by the assumed total height of the analysis cell. The fiber volume fraction of the top slice consisting of matrix only is equal to zero, and the thickness ratio of the top slice is equal to one minus the sum of the thickness ratio of the remaining slices.

The effective properties, effective inelastic strains and effective thermal strains of each slice are computed independently. The responses of each slice are combined using laminate theory to obtain the effective response of the corresponding lamina. Micromechanics equations are developed for those slices composed of both fiber and matrix material. The stresses in the slices composed of pure matrix can be computed using the matrix elastic properties and inelastic constitutive equations. The standard transversely isotropic compliance matrix (or isotropic in the case of the matrix) is used to relate the local strains to the local stresses in the fiber and matrix. Each slice is assumed to be in a state of plane stress on the global level, but out-of-plane normal stresses can exist in each subslice. Along the fiber direction, the strains are assumed to be uniform in each subslice, and the stresses are combined using volume averaging. The in-plane transverse normal stresses and the in-plane shear stresses are assumed to be uniform in each subslice, and the strains are combined using volume averaging. The out-of-plane strains are assumed to be uniform in each subslice. The volume average of the out-of-plane stresses in each subslice is assumed to be equal to zero, enforcing a plane stress condition on the global level for the slice.

An orthotropic compliance matrix is used to relate the strains (ϵ_{ij}) to the stresses (σ_{ij}) in each constituent. The addition of the inelastic strain components to the standard orthotropic elastic constitutive law facilitates the incorporation of inelasticity into the constitutive relations. For the fiber, which is assumed to be linear elastic, these components are neglected.

By combining the uniform stress and uniform strain assumptions with the constituent stress-strain relations, a system of four simultaneous equations results that can be solved for the unknown stresses in the subslices. The total strains and subslice inelastic strains are considered to be the known values in solving this problem. By substituting the subslice stresses back into the equations defining the uniform stress assumptions, the effective elastic constants, effective inelastic strains and effective thermal strains of the slice can be computed. By applying classical laminate theory at this point, the effective stiffness matrix, effective inelastic strains and effective thermal strains for the unit cell are computed. Laminate theory is applied once again to

obtain the effective properties and force resultants due to inelastic and thermal strains for the multilayered composite laminate. Further information on all of these procedures can be found in Goldberg¹³.

Simulation of Strain Rate Dependent Composite Deformation

To verify the micromechanics equations and the implementation of the polymer constitutive equations within them, a series of analyses have been carried out using a representative polymer matrix composite system that exhibits a strain rate dependent, nonlinear deformation response. The material examined consists of carbon IM7 fibers in the 977-2 toughened epoxy matrix discussed earlier. Longitudinal tensile tests were conducted on composite laminates with various fiber orientations. Tests were conducted at strain rates of about 5×10^{-5} /sec, about 1.0 /sec and about 400-600 /sec. Dog-bone shaped specimens were used with a gage length of approximately 0.9525 cm. The low strain rate testing was conducted using an Instron hydraulic testing machine. The high strain rate tests were conducted using a tensile split Hopkinson bar apparatus.

The IM7/977-2 composite has a fiber volume ratio of 0.60. The material properties used in this study for the IM7 fiber include a longitudinal modulus of 276 GPa, a transverse modulus of 13.8 GPa, a longitudinal Poisson's ratio of 0.25, a transverse Poisson's ratio of 0.25 and an in-plane shear modulus of 20.0 GPa. These properties are as given in Gates, et al¹⁷, with the exception of the value for the transverse Poisson's ratio was taken from Murthy, et al¹⁸ based on representative carbon fiber data. The material properties of the 977-2 resin are as given before.

Experimental and computed longitudinal tensile stress-strain curves for two laminate configurations ($[45^\circ]$ and $[\pm 45^\circ]_s$) of the IM7/977-2 material are shown in Figure 4 and Figure 5. These laminate configurations were chosen due the pronounced nonlinearity and strain rate dependence observed in the experimental results. Five fiber slices were used in the portion of the unit cell which was analyzed. This value was found to yield sufficiently converged answers. In Figure 4, results for the $[45^\circ]$ laminates at strain rates of 4.75×10^{-5} /sec, 1.2 /sec and 405 /sec are shown. In Figure 5, results for the $[\pm 45^\circ]_s$ laminates at strain rates of 9×10^{-5} /sec, 2.1 /sec and 604 /sec are shown.

As can be seen in the figures, the analytical model captures the strain rate dependence and nonlinearity observed in the experimental stress-strain curves. For the low and moderate strain rate curves for both laminates and the high strain rate curve for the $[45^\circ]$ laminate, the comparison between the experimental and analytical results is reasonably good. The stresses at

the moderate strain rate for the $[\pm 45^\circ]$, laminate are somewhat overpredicted and the stresses at the low strain rate for the $[45^\circ]$ laminate are somewhat underpredicted for reasons which are clear at this time. For the $[\pm 45^\circ]$, laminate at high strain rates, the stresses are significantly overpredicted, indicating that there may have been some damage in the experimental specimens which is not predicted with the current analytical model. Alternatively, there could be an error in the material constants. The specific causes for the discrepancies need to be investigated further.

Conclusions

A set of constitutive equations have been developed to analyze the strain rate dependent, nonlinear deformation of polymeric matrix materials, including hydrostatic stress effects. The tensile and shear deformation response of a representative polymer over a range of strain rates have been successfully predicted. The constitutive equations have been implemented within a strength of materials based micromechanics approach in which the unit cell is subdivided into a set of independently analyzed slices. The micromechanics technique was used to predict the strain rate dependent deformation of a representative polymer matrix composite for two fiber orientations. Overall, the experimental stress-strain curves were accurately predicted using the model, with some discrepancies for the high strain rate results which need to be investigated further.

References

1. Anonymous: LS-DYNA Keyword User's Manual, Version 950. Livermore Software Technology Corporation, Livermore, CA, 1997.
2. Wineman, A.S.; and Rajagopal, K.R.: Mechanical Response of Polymers. Cambridge University Press, New York, 2000.
3. Weeks, C.A.; and Sun, C.T.: "Modeling Non-Linear Rate-Dependent Behavior in Fiber-Reinforced Composites." *Composites Science and Technology*, Vol. 58, pp. 603-611, 1998.
4. Thiruppukuzhi, S.V.; and Sun, C.T.: "Testing and modeling high strain rate behavior of polymeric composites." *Composites Part B*, Vol. 29B, pp. 535-546, 1998.
5. Bordonaro, C.M.: "Rate Dependent Mechanical Behavior of High Strength Plastics: Experiment and Modeling." PhD Dissertation, Rensselaer Polytechnic Institute, Troy, New York, 1995.
6. Li, F.Z.; and Pan, J.: "Plane-Stress Crack-Tip Fields for Pressure-Sensitive Dilatant Materials." *Journal of Applied Mechanics*, Vol. 57, pp. 40-49, 1990.
7. Chang, W.J.; and Pan, J.: "Effects of Yield Surface Shape and Round-Off Vertex on Crack-Tip Fields for Pressure-Sensitive Materials." *International Journal of Solids and Structures*, Vol. 34, pp. 3291-3320, 1997.
8. Hsu, S.-Y., Vogler, T.J.; and Kyriakides, S.: "Inelastic behavior of an AS4/PEEK composite under combined transverse compression and shear. Part II: modeling." *International Journal of Plasticity*, Vol. 15, pp. 807-836, 1999.
9. Ward, I.M.: Mechanical Properties of Solid Polymers. John Wiley and Sons, New York, 1983.
10. Khan, A.S.; and Huang, S.: Continuum Theory of Plasticity. John Wiley and Sons, Inc., New York, 1995.
11. Goldberg, R.K.; Roberts, G.D.; and Gilat, A.: Incorporation of Mean Stress Effects Into the Micromechanical Analysis of the High Strain Rate Response of Polymer Matrix Composites. NASA/TM-2002-211702, 2002.
12. Bodner, S.R.: Unified Plasticity for Engineering Applications. Kluwer Academic/Plenum Publishers, New York, 2002.
13. Goldberg, R.K.: Computational Simulation of the High Strain Rate Tensile Response of Polymer Matrix Composites. NASA/TM-2002-211489, 2002.
14. Whitney, J.M.: "A Laminate Analogy for Micromechanics." *Proceedings of the American Society for Composites Eighth Technical Conference*, G.M. Newaz, ed., Technomic Publishing Co., Lancaster, PA, pp. 785-794, 1993.
15. Greszczuk, L.B.: "Interfiber Stresses in Filamentary Composites." *AIAA Journal*, Vol. 9, pp. 1274-1280, 1971.
16. Mital, S.K.; Murthy, P.L.N.; and Chamis, C.C.: "Micromechanics for Ceramic Matrix Composites Via Fiber Substructuring." *Journal of Composite Materials*, Vol. 29, pp. 614-633, 1995.

17. Gates, T.S.; Chen, J.-L.; and Sun, C.T.: "Micromechanical Characterization of Nonlinear Behavior of Advanced Polymer Matrix Composites." Composite Materials: Testing and Design (Twelfth Volume), ASTM STP 1274, R.B. Deo and C.R. Saff, eds., ASTM, pp. 295-319, 1996.
18. Murthy, P.L.N.; Ginty, C.A.; and Sanfeliz, J.G.: Second Generation Integrated Composite Analyzer (ICAN) Computer Code. NASA TP-3290, 1993.

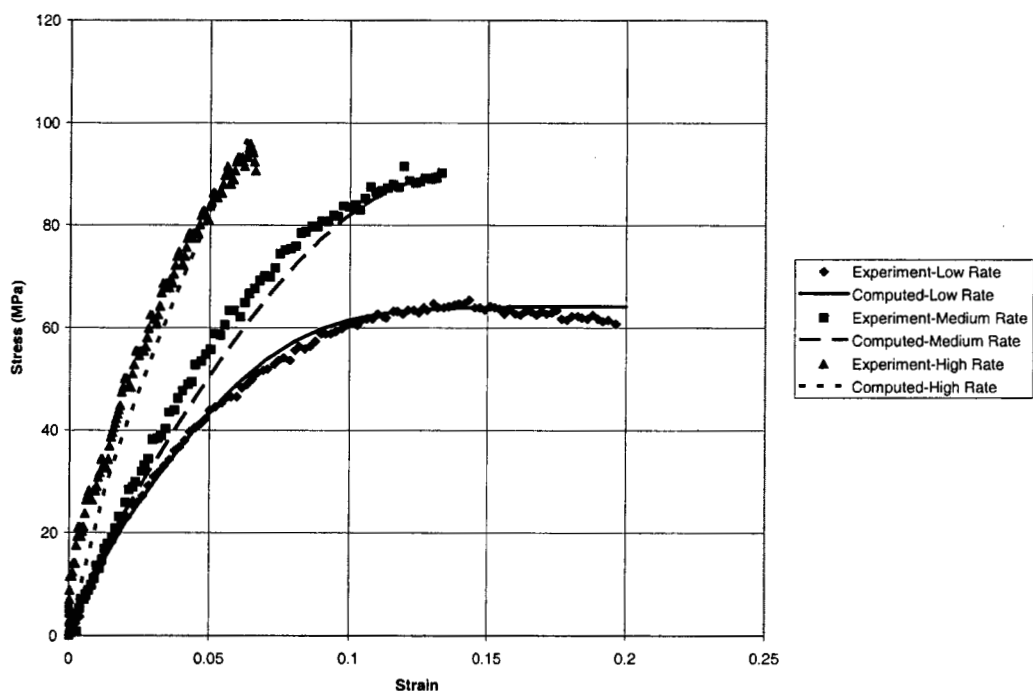


Figure 1: Experimental and computed shear stress-shear strain curves for 977-2 resin at strain rates of 9×10^{-5} /sec (Low Rate), 1.9 /sec (Medium Rate) and 518/sec (High Rate).

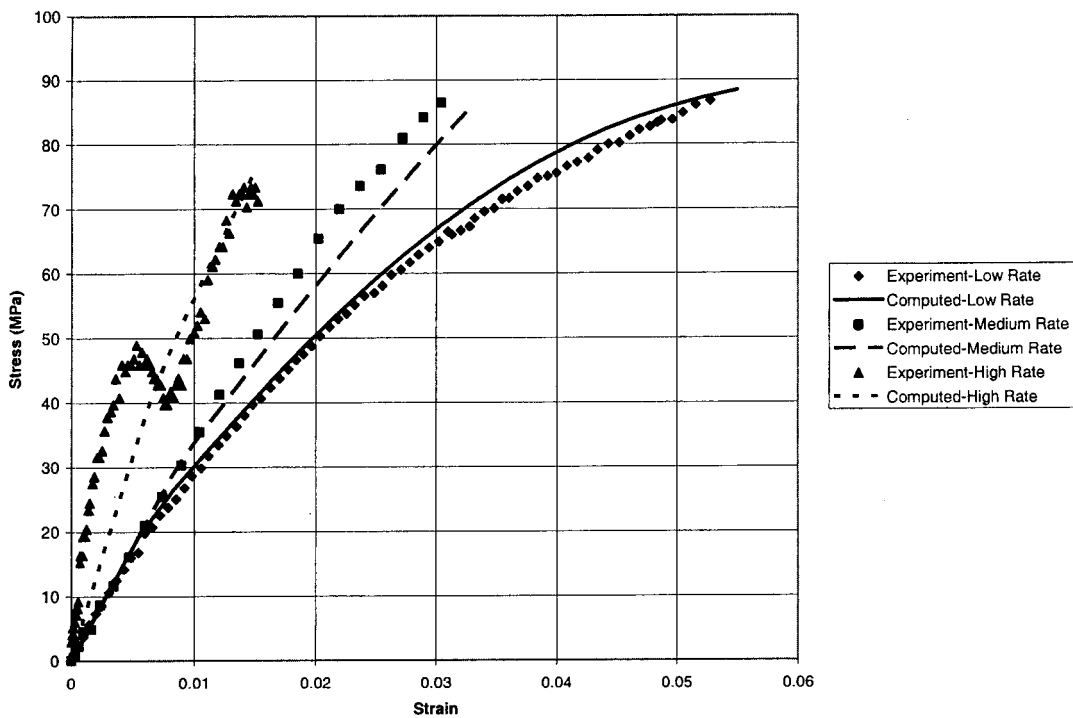


Figure 2: Experimental and computed tensile stress-strain curves for 977-2 resin at strain rates of 5.7×10^{-5} /sec (Low Rate), 1.9 /sec (Medium Rate) and 365 /sec (High Rate).

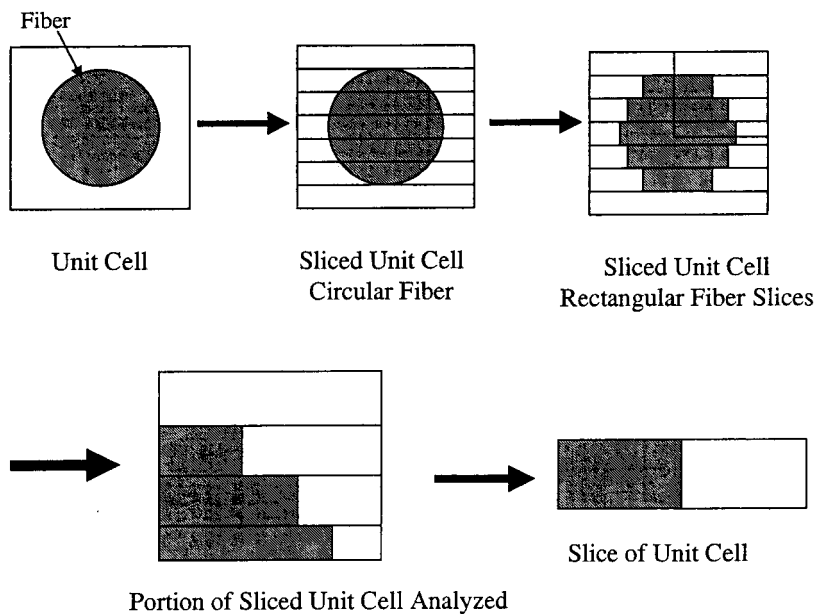


Figure 3: Schematic showing relationship between unit cell and slices for micromechanics.

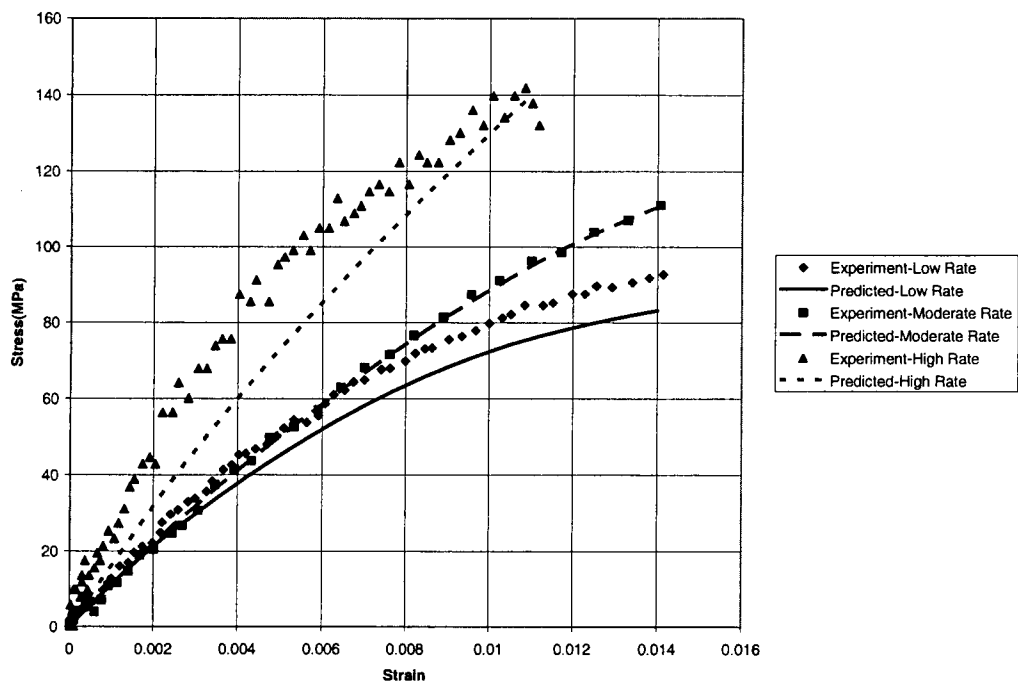


Figure 4: Experimental and predicted results for IM7/977-2 [45°] laminates at strain rates of 4.7×10^{-5} /sec (Low Rate), 1.2 /sec (Medium Rate) and 405 /sec (High Rate).

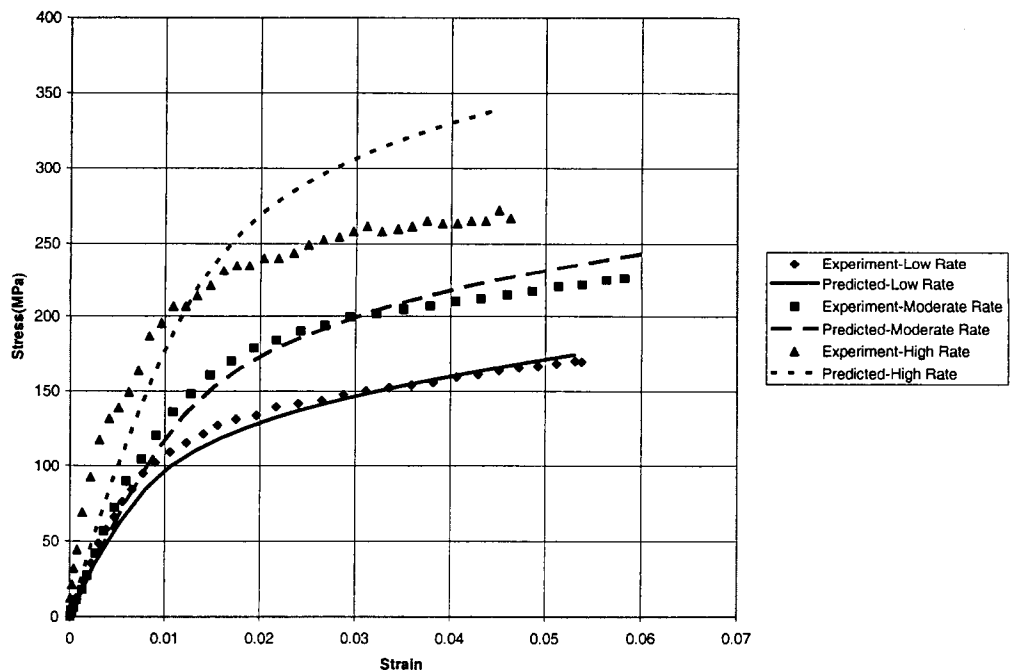


Figure 5: Experimental and predicted results for IM7/977-2 [±45°]_s laminates at strain rates of 9×10^{-5} /sec (Low Rate), 2.1 /sec (Moderate Rate) and 604 /sec (High Rate).